

THE EFFECT OF PHASE TRANSITIONS IN Al_2O_3 -SiC-BN ZIRCONIA DOPED SYSTEM ON THE MECHANICAL PROPERTIES OF CERAMICS

V.G. Konakov^{1,2,3}, E.N. Solovyeva^{1,2}, I.Yu. Archakov^{1,2,4} and S.N. Golubev¹

¹Scientific and Technical Center "Glass and Ceramics", St. Petersburg, Russia

²Institute of Problems of Mechanical Engineering, Russian Academy of Sciences, St. Petersburg, Russia

³Department of Chemistry, St. Petersburg State University, Staryi Peterhof, St. Petersburg, Russia

⁴St. Petersburg University, Staryi Peterhof, St. Petersburg, Russia

Received: October 13, 2013

Abstract. Thermal analysis of ternary Al-BN-SiC batch aimed for the production of nanomodified functional Al_2O_3 -BN-SiC ceramics and the analysis of binary systems and individual compounds forming the above system were performed. It was shown that powders dispersion and samples pretreatment (pressing, heating in air, and vacuum annealing) affect thermal behavior of the samples. The nature of endothermic and exothermic effects as well as peculiarities of weight changes during heating-cooling cycles are discussed. The information for ternary system samples is compared with the data obtained for samples modified by nano-sized zirconia powder. As a result of the study, the conclusion on the suitability of the chosen composition for the manufacturing of nanomodified functional ceramics is stated.

1. INTRODUCTION

Introduction of thermally stable inorganic nanosized particles into ceramics and metal-ceramic (cermet) materials and, especially, the effect of this doping on the mechanical, thermal, and other properties of such nano-modified materials is, at the moment, poorly studied. However, these functional materials are treated as being very perspective in power engineering, air- and space industries, turbine technologies, etc.; as an example, the use of such materials in the ceramic turbine production [1] can be mentioned. A number of recent papers describes the specific behavior of thermally stable inorganic nanosized particles in the wide temperature range typical for the processes of nano-modified ceramics/cermets manufacturing [2-4], as well as the purposeful changes in the nano-modified materials properties [5].

This paper reports the investigation of Al_2O_3 -SiC-BN system doped by nanosized ZrO_2 powder,

Corresponding author: Vladimir Konakov, e-mail: glasscer@yandex.ru

stabilized by 9 mol.% of Y_2O_3 (YSZ). Since the mechanical properties of Al_2O_3 -SiC-BN in the temperature range from 25 to 1000 °C are thoroughly studied [6], these data can be used in order to understand the doping effect. Yttrium stabilized zirconia was chosen as a nanomodifier since its addition possess [2] to modify the required mechanical and thermal properties of final ceramics.

2. SAMPLE SYNTHESIS

Synthesis of Al_2O_3 -SiC-BN samples was reported in detail in [7]; briefly, it can be described as follows: a batch consisting of Al, SiC, and BN was mechanically activated in a planetary mill (Pulverizette 6); then, the mechanoactivated batch was pressed into \varnothing 50 mm cylindrical billets with 35 mm in height. The billets were thermally treated in a vacuum furnace at 1200-1250 °C for 2 hours, as a result, cer-

met samples were manufactured. At the next step, the billets were cut into samples for mechanical tests; these samples were oxidized at 1250 °C in air for 120 hours, this oxidation was the ending step of the transformation of the batch into final Al_2O_3 -SiC-BN ceramics.

Yttrium-stabilized ZrO_2 nanosized particles were synthesized using sol-gel reverse precipitation method; as it was shown in [8,9], it is possible to manufacture nanoparticles of required size in the range 50-500 nm varying such process parameters as pH, solution concentration, and temperature. Thermal evolution of ZrO_2 stabilized by 9 mol.% Y_2O_3 nanoparticles was studied in detail in [3,9].

To produce nano-modified ceramics, YSZ nanoparticles were added into the batch just before mechanical activation step; the rest synthesis procedure was the same. Basic intermediate products (batch, cermet) and the final ceramic samples were taken for thermal (Netzsch STA 449 F1 Jupiter) and XRD (SHIMADZU XRD-6000) analysis.

3. RESULTS AND DISCUSSION

3.1. Phase transformations in individual components and binary mixtures

3.1.1. Individual components

SiC, BN, and Al powders were studied at the first step of the work; experiments were carried out in the temperature range 50 – 950 °C.

Let us discuss the thermal analysis data in more detail. Thermograms characterizing silicon carbide powder in the temperature range 50 – 950 °C have no peculiarities; this fact proves the absence of phase transitions and chemical reactions with ambience during heating in the above temperature range; this data agrees with the reference information [10]. Thus, chemical and thermal stability of silicon carbide as well as the stability of its phase composition at 50 – 950 °C was confirmed.

Similar behavior was shown for boron nitride powder (Fig. 1, DTA and TG, lines #2). However, it is well known that preliminary treatment of the material, in particular, its mechanical activation as a result of milling in a planetary ball mill, could affect physical and chemical properties of the material. To check these hypothesis, the following experiment was carried out. BN powder was milled and mechanically activated during the additional milling in the Pulverisette 6 planetary ball mill; the milling conditions were as follows: agate vessel with agate

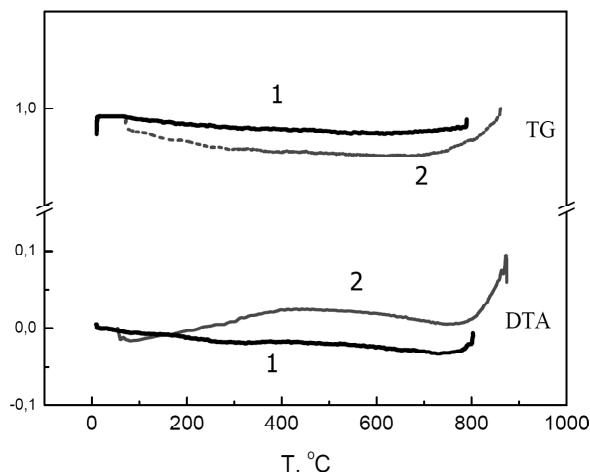
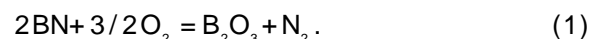


Fig. 1. The results of thermal analysis (DTA and TG curves) for the boron nitride powder used as one of the initial components during nano-modified functional ceramic material synthesis. Curves #1 - mechanically activated powders, curves #2 - initial BN powder.

balls; rotation rate was 300 rpm, duration of the milling was 250 minutes with 5 reverse changes. Thermal analysis was repeated for mechanically activated BN powder (lines # 1 in Fig. 1). As seen from the comparison of DTA and TG curves detected for initial and mechanically activated powders, mechanical activation did not affect the behavior of individual boron nitride.

Some researchers claimed the possibility of boron nitride oxidation at temperature ~ 850 °C as a result of interaction with the atmospheric oxygen, Reaction (1), the heat effect of this reaction is estimated to be ~ -37 kJ/mole:



However, such a significant exothermic effect should clearly manifest itself on the DTA curve of the studied sample; data presented in Fig. 1 did not support the discussed assumption on possible boron nitride oxidation.

The study of physical and chemical processes occurring during the heating of individual aluminum powder was very interesting, since, in contrast to SiC and BN powders, significant effects conditioned by aluminum melting were expected here. Aluminum samples with different powders dispersity and preliminary treatment history were studied, the results of their thermal analysis is demonstrated in Fig. 2.

This figure shows the DTA curves obtained for the initial powder (Fig. 2a), and for the fractions separated using the sieves with 80, 40, and 10 μm

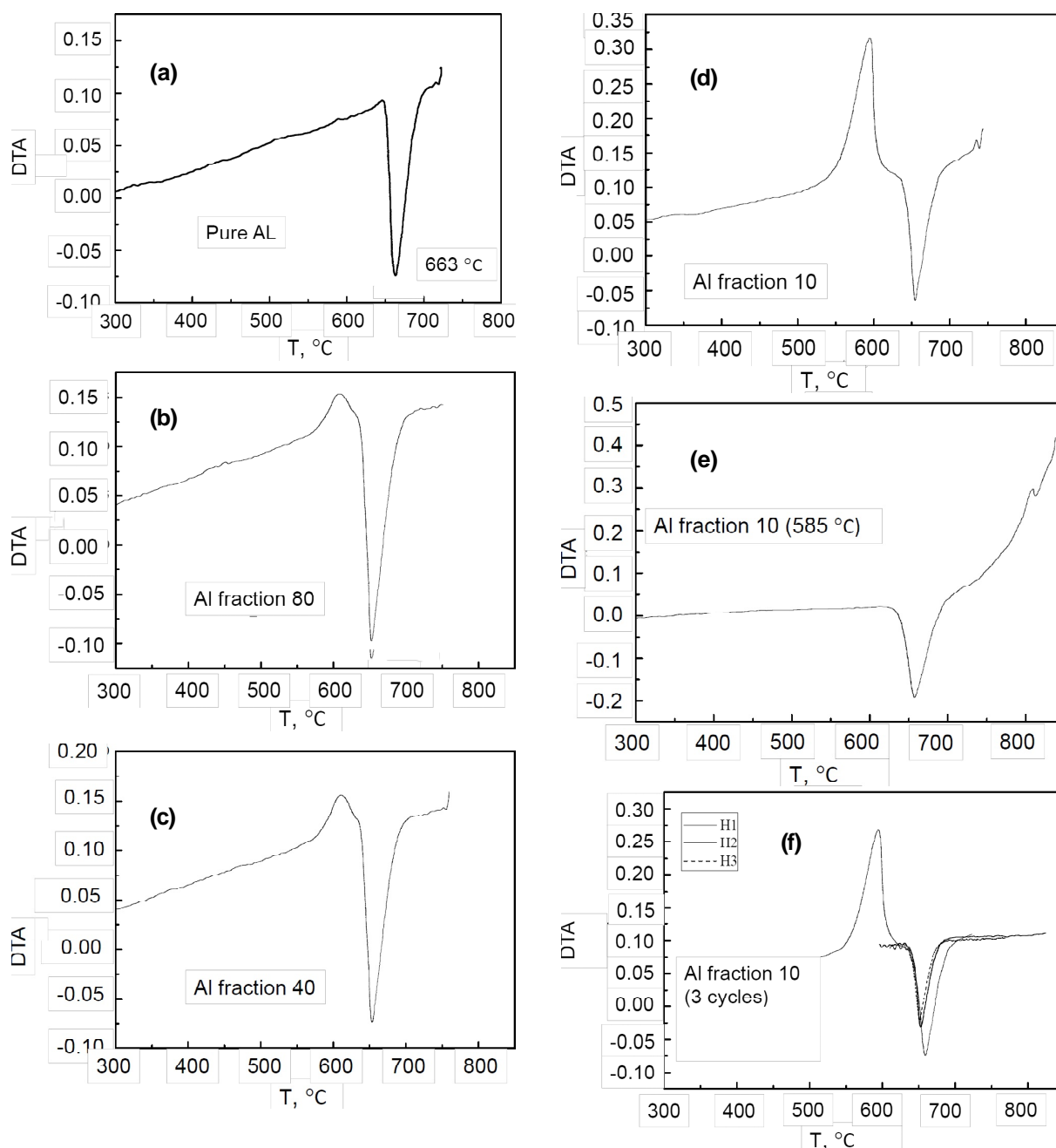


Fig. 2. The results of thermal analysis (DTA curves) for aluminum powders.

cells, i.e. powders with the average particle sizes less than 80, 40, and 10 μm , Figs. 2b, 2c, and 2d, respectively. Clearly indicated endothermic effect can be observed for all samples at temperatures 663–670 $^{\circ}\text{C}$, it corresponds to the metal aluminum melting.

Samples of ultra-fine powders (Figs. 2b, 2c, and 2d) demonstrate exothermic effect in the temperature range 580–600 $^{\circ}\text{C}$. Note that this effect is typical for ultrafine powders only, bulk aluminum (see Fig. 2a) does not show any traces of the effect. In addition, the enthalpy of this exothermic effect depends on powder dispersity: the less is the particle

size in the powder, the higher is the enthalpy effect. Indeed, comparison of Figs. 2c and 2d proves that the enthalpy effect for the powder with 10 μm fraction is twice higher than that for the powder with 40 μm fraction. Since the discussed exothermic effect was more evident for the aluminum powder with 10 μm fraction, some further experiments with the thermally treated powder with 10 μm fraction were performed. The repeated heating of the powder did not reproduce the discussed exothermic effect. Fig. 2e presents the results of thermal study of the aluminum powder with 10 μm fraction heated at 585 $^{\circ}\text{C}$ for 1 hour; exothermic effect is not observed here. Fig. 2f

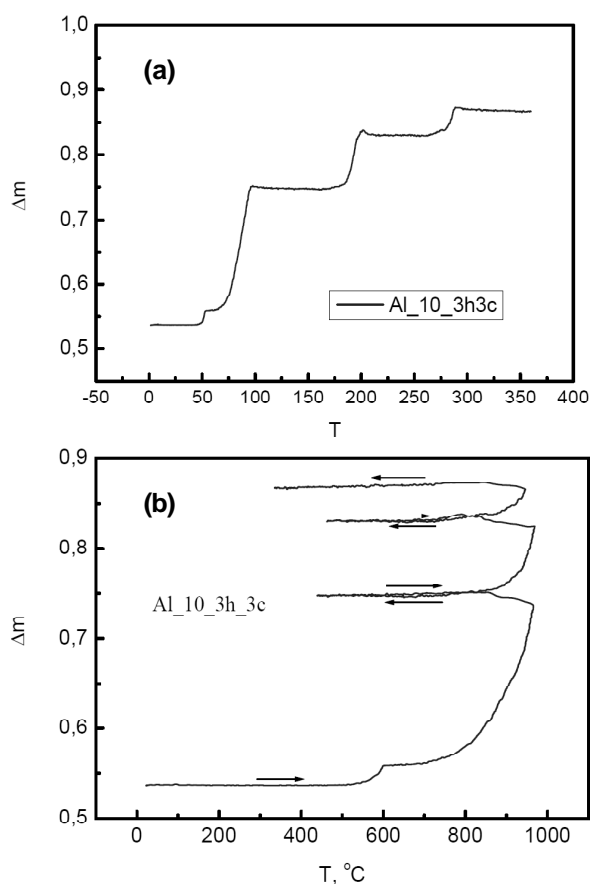


Fig. 3. Mass changes during the heating of the aluminum sample with the powder fraction 10 μm .

depicts the thermograms obtained during triple serial pass of the aluminum sample through 500-750 $^{\circ}\text{C}$ temperature interval (initial aluminum powder with 10 μm fraction, sample without any thermal treatment). The first pass (curve 1 in Fig. 2f) is identical to that presented in Fig. 2d; however, exothermic effect is not observed both on the second and third pass curves, curves 2 and 3 in Fig. 2f, respectively. It should be also mentioned that the value of endothermic effect attributed to aluminum melting is somehow less for second and third pass curves comparing to the value obtained during primary pass.

To understand the nature of exothermic effect at 580-600 $^{\circ}\text{C}$, we've tried to find the dependence between the enthalpy values of endothermic and exothermic effects and the change in the sample weight during heating (TG curves). Fig. 3 demonstrates the sequence of sample weight changes at serial sample heating, horizontal line here corresponds to cooling. Note, that these calculations were performed accounting for the following: calibration was performed using the reference data on the melting enthalpy of pure (99.999) alumi-

num at 660.3 $^{\circ}\text{C}$ – 397 J/g. The second reference point was the measurement of the heat effects of K_2CrO_4 polymorphous transitions at 666 $^{\circ}\text{C}$; the enthalpy of this transition was 10 kJ/mole. According the results obtained during these calibration experiments, the error in the determination of the enthalpy values within the applied approach was estimated as being less than 15%.

According to the reference data, the enthalpy of the alumina (Al_2O_3) formation at 627 $^{\circ}\text{C}$ is -1609 kJ/mole. Assuming the exothermic effect at 585 $^{\circ}\text{C}$ as being also connected with the alumina formation due to the sample interaction with the atmosphere oxygen, Reaction (2):



It can be possible to estimate the mass of the formed alumina and, in turn, the change in the sample weight due to the aluminum oxide formation. However, the increase in the sample weight calculated via Reaction (2) using the data on the heat constituent part of the effect (i.e. the mass of oxygen reacting with aluminum to form proper amount of Al_2O_3) is less than the mass change determined from the TGA curve. Note that further heating is characterized by the significant sample weight increase that is likely due to the aluminum oxidation, however, no exothermic effects are detected at further sample heating. This fact indicates that the exothermic effect registered at temperature ~ 585 $^{\circ}\text{C}$ is not the result of oxidation reaction (3) (or, may be, only some part of it can be assumed as being due to the above reaction), but can attributed to some alternative process. One can assume such process as the release of the surface energy yielding from the particles enlargement that, in turn, leads to the decrease in the integral sample surface. This assumption was proved by the additional study of particle-size distributions (Horiba LA-950) and XRD pattern analysis (Shimadzu XRD-6000). According to PSD data, the initial fraction 10 μm aluminum powder was characterized by the average particle size being less than 10 μm and the maximal particle size here was less than 15 μm . Particle-size distribution measurements of the same powder after thermal analysis indicate that the significant part of the powder particles have much higher dimensions (up to 300 μm). XRD pattern analysis also shows that the powder crystallinity increases with temperature increase and/or heat treatment duration.

The amount of aluminum melted at 660 $^{\circ}\text{C}$ was estimated using TG data; for comparison, the cal-

culated data were normalized accounting for heating conditions and sample weight. These estimates show that such an amount of melted aluminum for 40 and 80 μm fractions was lower than that estimated for initial sample; in contrast, the amount of melted aluminum calculated for 10 μm fraction was higher than that for initial sample. However, this exceed lies within the error that can result from the above discussed uncertainty range of 15%. Indeed, calculations performed for triple cycle of heating-cooling (we should remind that the endothermic effect attributed to aluminum melting registered for second and third pass through the temperature range 500-750 $^{\circ}\text{C}$ was less than that for the first pass) result in the amount of melted aluminum lower than that for initial sample. Above results can be summarized as follows. The lower amounts of melted aluminum for samples with higher dispersity (80, 40, and 10 μm) can be the result of preliminary aluminum consumption due to the oxidation Reaction (3); the results obtained for 10 μm fraction single pass lie within the error range due to the measurement uncertainties.

Thus, the basic result of thermal analysis is the fact that exothermic effect at temperatures $\sim 585^{\circ}\text{C}$ is the result of energy release from the surface of the ultrafine aluminum powder. It is very interesting that this effect was registered in a rather narrow temperature range 550-600 $^{\circ}\text{C}$. The higher is the powder dispersity, the more evident is the discussed exothermic effect; its value is even comparable with endothermic effect attributed to aluminum melting; moreover, for the sample with highest dispersity (10 μm fraction), the effect of energy release exceeds the effect of aluminum melting. The second important conclusion is the fact that the enthalpy of the endothermic effect resulting from aluminum melting decreases in the repeated passes through the melting temperature, while the exothermic effect manifests itself only once after the first heating up to 585 $^{\circ}\text{C}$, it is not registered in second and third passes. In addition, particle-size measurements proves that heating up to 900 $^{\circ}\text{C}$ gives rise to the significant increase in the number of large particles with the sizes 10-15 times higher than those typical to initial powders.

3.1.2. Binary samples

The first system studied was boron nitride - aluminum system, mixtures of initial powders with the following compositions 40%Al-60%BN, 50%Al-50%BN, 60%Al-40%BN, and 70%Al-30%BN (mole%) were taken as the samples. Note that these

samples were the mechanical mixture of the initial BN reagent with fraction 10 μm Al powder, thermal behavior of this fraction was studied in detail, see previous Section. In addition to mechanical powders, two series with some prehistory were investigated. The first series includes pellets formed from the above listed mixtures using the hydraulic press, the compacting pressure was 8 ton/cm², pressing duration was 10 minutes. The second series consists of the same pellets thermally treated in vacuum furnace at 1000 $^{\circ}\text{C}$ for 2 hours.

Thermal analysis results for these samples, GTA and TG curves, are presented in Figs. 4a-4d. Curve 1 in all figures corresponds to mechanical mixture of the powders; curve 2 shows the results registered for compacted pellets; curve 3 describes the behavior of the heat treated pellets. Let us discuss these results in more detail.

Comparing the shape of curve 1 in Fig. 4a with the data obtained for individual fraction 10 μm aluminum, see Fig. 2, one can conclude that boron nitride addition does not significantly affect the curve behavior. Indeed, similar exothermic effect attributed above to the energy release due to the powder dispersity decrease and similar endothermic effect resulting from aluminum melting are evidently seen in Fig. 4a. Note that the increase in boron nitride content up to 40, 50, and 60 mole %, Figs. 4b, 4c, and 4d, respectively, also did not affect the general behavior of DTA and TG curves of the binary system.

As seen from the analysis of the thermograms obtained for the pressed pellets (curves in Figs. 4a-4d), compacting significantly affects the thermal behavior of the samples. The comparison of the exothermic effect value in pressed pellets with those in the mechanical mixture of the powders indicates the evident decrease of the effect in all compacted samples. Some tendency of the decrease in the exothermic effect value with the increase in boron nitride content can be claimed, but this suggestion requires additional experimental support.

Exothermic effect peak is not registered in the curves obtained for pellets heat treated at 1000 $^{\circ}\text{C}$, curves 3 in Figs. 4a-4d; this fact agrees with the data reported for individual fraction 10 μm aluminum in the previous Section. So, it can be stated that the exothermic effect typical for the DTA curves of the Al-BN system, similar to individual aluminum case, is due to the energy release resulting from the powder dispersity decrease, i.e. the increase in the average and maximal particle size; primarily, this effect corresponds to aluminum part of the system. Results obtained for compacted and high temperature treated powders support this conclusion.

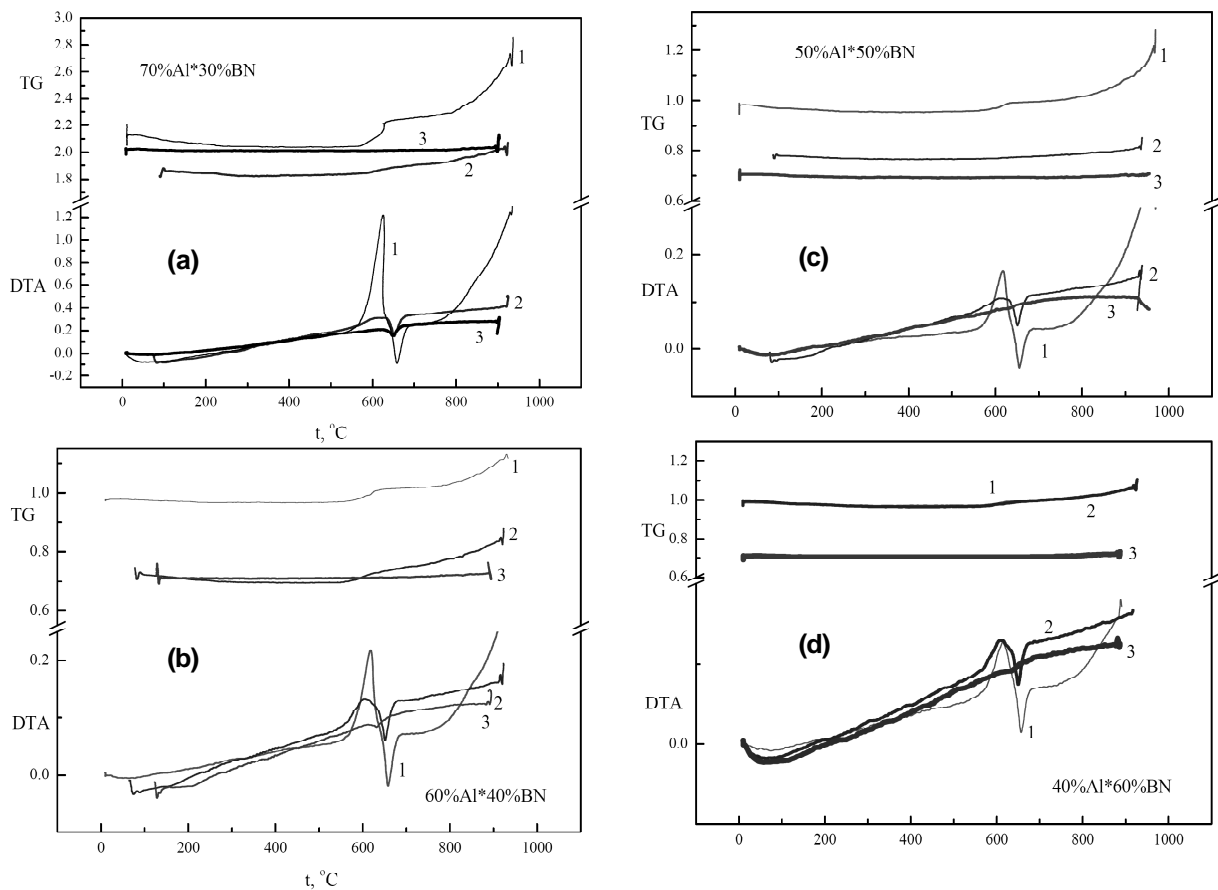


Fig. 4. Thermograms (DTA and TG curves) for the heating of the Al-BN system samples, mole%: (a) 70% Al-30% BN, (b) 60% Al-40% BN, (c) 50% Al-50% BN, and (d) 40% Al-60% BN, in all figures curve 1 corresponds to mechanical mixture of the powders, curve 2 – pressed pellets, curve 3 – heat treated pellets.

The next studied system was aluminum – silicon carbide system, samples with 10%Al90%SiC, 25%Al75%SiC, 50%Al50%SiC, 75%Al25%SiC, and 90%Al10%SiC (mole%) were investigated. Similarly to Al-BN system discussed above, fraction 10 μ m Al was used as aluminum-containing component. Two kind of initial SiC powders were used: fraction 7 – fraction with the average particle size of 7 μ m, and fraction 14 – fraction with the average particle size of 14 μ m. Binary compositions here were powder mixtures prepared as follows: initial reagents wetted by ethanol were grinded in agate mortar with following drying at room temperature for 20 hours.

Fig. 5 demonstrates the thermal analysis results obtained for the Al-SiC system in the temperature range 50-950 $^{\circ}$ C.

Fig. 5a illustrates the increment in the sample weight. The total increment marked as T is the weight increment (m_T) during the whole heating up to 950 $^{\circ}$ C – cooling down to room temperature cycle, while the first weight increment (I) – is the mass increase (m_I) after the effect that corresponds to

the evident exothermic peak at 580-600 $^{\circ}$ C; numbers 7 and 14 indicate the silicon carbide fraction. For better understanding of the thermogram curves type, a curve typical for the samples of Al-SiC system is presented in Fig. 5b, this is a curve registered for the sample with 50%Al50%SiC composition, SiC fraction was 14.

All Al-SiC samples studied were characterized by the sample weight increase (Fig. 5a), we've assumed this fact as being due to the oxidation of the system components. As seen from Fig. 5a, oxidation level that corresponds directly to the sample total weight increment m_T at heating up to 950 $^{\circ}$ C, significantly depends on sample composition and SiC fraction. The oxidation level is practically constant for samples with SiC composition less than 50%; moreover, data for fractions 7 are 14 and quite similar. At further SiC content increase, oxidation level for fraction 14 SiC sample is of the same order, while sample with fraction 7 SiC shows the significant increase. Note that such a behavior, i.e. the significant dependence of the oxidation level

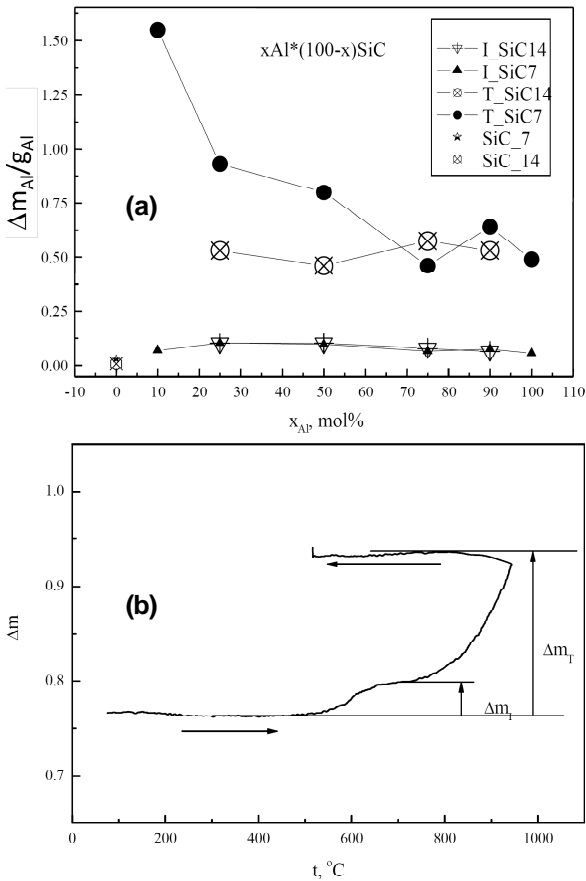


Fig. 5. Thermal analysis results for Al-SiC system: (a) the weight increment – first (I) and total (T) and (b) typical thermogram demonstrating the behavior of Al-SiC system samples (50%Al50%SiC, fraction 14 SiC sample).

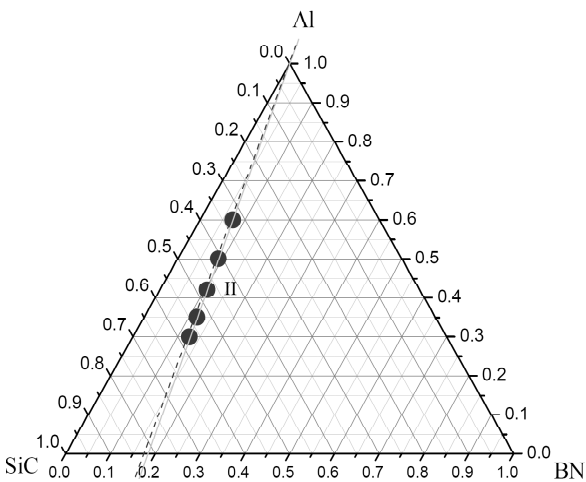


Fig. 6. Compositions of Al-SiC-BN system studied in the present work.

on sample composition was not typical for Al-BN system. On the other hand, this effects is undoubtedly related to the dispersity of silicon carbide; thus, it was reasonable to attribute it to the reaction of silicon dioxide (SiO_2) formation during SiC oxida-

tion. We should also remind that thermograms, obtained for individual silicon carbide, see Section 1, have no peculiarities in the temperature range of the present study; this means that the oxidation of pure silicon carbide is less active than that for the carbide mixed with ultra-fine aluminum. So, it can be stated that system components even affect each other oxidation behavior.

It should be also noted that the study of the first weight increase (m_1) values as well as the values of the first weight increment of the individual silicon carbide of both fractions marked as SiC7 and SiC14 in Fig. 5a did not show any significant difference caused by sample composition and SiC dispersity.

3.2 Ternary systems and batch samples used to manufacture nanomodified ceramics

The next step of this work was the study of ternary aluminum- boron nitride – silicon carbide (Al-BN-SiC) system; since the complete system investigation is a task requiring a great amount of work, we've restricted ourselves by the composition region that is basic for functional nanomodified ceramics; this region is depicted in Fig. 6. It should be mentioned, that the analysis of literature and patent information, see e.g. [11-13] indicates silicon nitride (Si_3N_4) and individual boron (B) as the most expected intermediate compounds forming during the synthesis of functional ceramic material from the initial reagents mixture.

As shown in Fig. 6, compositions lying on the section with the SiC/BN mole fraction ratio of 4.514 containing 30, 35, 42, 50, and 60 mole % Al were studied. Aluminum fraction 10 μm was used for samples preparation since all thermal effects for this fraction were more evident than in systems with lower dispersity. Silicon carbide 7 fraction that demonstrates the dependence of weight increment on binary system composition in Al-SiC system was taken as silicon carbide initial reagent. Boron nitride was 10 μm fraction, this fraction was used in all our previous studies. Generalized data on thermal investigations for ternary system is presented in Figs. 7 and 8.

Analysis of the data presented in Fig. 7 gives the opportunity to make some conclusions on the suitability of the chosen batch composition for the production of nanomodified functional ceramics. As seen from Fig. 7, the value of endothermic effect normalized on 1 g of aluminum in the initial powder mixture is similar for all compositions studied, while the exothermic effect value has an extremum (maxi-

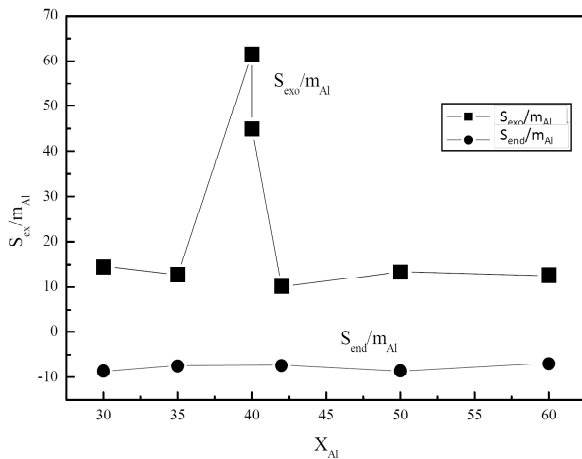


Fig. 7. The values of endo- and exothermic effects in Al-BN-SiC system according DTA data.

num) at aluminum content corresponding to the composition chosen for nanomodified ceramics manufacturing.

Analysis of the weight changes thermograms, Fig. 8, calculated on the base of the results presented in Fig. 7 also indicates the peculiarities in the mass changes in the temperature range 580-600 °C (m_1) as well as in the total mass increment during the whole heating-cooling cycle (m_T); these data can be compared with the information for Al-SiC system shown in Fig. 5. Similarly to the energy effects, Fig. 7, data on mass changes proves that the most intensive components interaction takes place in case of ternary system composition chosen for nanomodified ceramics manufacturing. These interactions provide the required physical and chemical properties of the final ceramics: thermal stability, chemical stability, and permanence of phase composition at high temperatures.

3.3. Thermal analysis of the nanomodified functional ceramics

The specific task of thermal analysis was the study of the nano-modifies effect on the thermodynamic properties of the initial materials used for the nanomodified functional ceramics production. A set of experiments was carried out, their results will be presented in our following publications.

Here we'll present the comparison of the thermal analysis data for one of the batch compositions based on ternary Al-BN-SiC system with the same composition batch modified by nano-sized zirconia powder. Fig. 9 demonstrates DTA and TG curves for the 14%BN26%SiC60%Al batch composition (mole %); billets for thermal analyses were

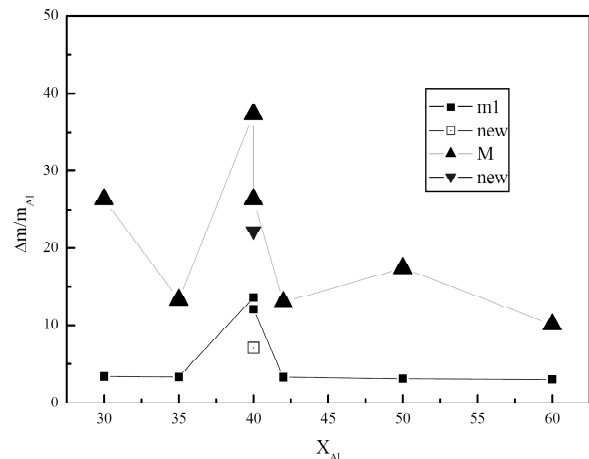


Fig. 8. Weight changes of the ternary Al-BN-SiC system samples recalculated to 1 g of aluminum in the initial powders mixture.

pressed under 22 ton/cm² (here and after –sample #100), as seen from the figure, these curves are quite close to those obtained for ternary Al-BN-SiC system. Fig. 10 presents the same curves registered for the billet compacted from sample # 100 batch and nano-sized zirconia powder, 95 wt.% and 5 wt.%, respectively.

As seen from Figs. 9 and 10, thermal analysis of the samples nanomodified by zirconia show the same major effects caused by aluminum melting and corresponding crystallization at cooling; these effects were observed earlier for individual aluminum, aluminum-containing binary mixtures and ternary Al-BN-SiC system. However, a new exothermic effect with maximum at ~ 650 °C is observed for nanomodified samples; it is registered just after the peak typical for the first heating pass for all studied systems including pure ultrafine aluminum. The value of this new exothermic effect is comparable with the value of the previously observed exothermic effect. Similarly to the conclusions presented in the previous Section, the presence of the new exothermic effect supports the statement that nanomodifier addition to ternary Al-BN-SiC system batch gives rise to additional interactions between system components; in turn, this fact makes possible purposeful modification of the required final ceramics properties.

4. CONCLUSIONS

Thermal analysis performed for individual aluminum, boron nitride, and silicon carbide powders, their binary systems, ternary Al-BN-SiC samples and same samples modified by nanosized zirconia powder demonstrates that:

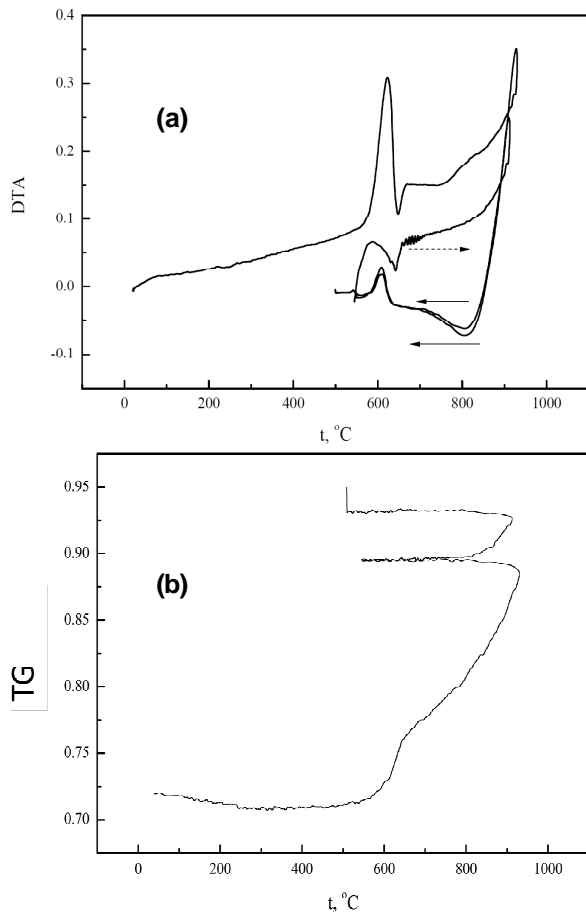


Fig. 9. Thermograms of the 14%BN26%SiC60%Al (mole %) sample batch: a – DTA curves, (b) – TG curves.

1. Dominant thermal effects in non-modified samples are due to processes occurring with individual aluminum: melting at heating, crystallization at cooling, oxidation.
2. Specific effect is observed at 550-600 °C, we've attributed it to the release of the energy due to decrease in powder dispersity, i.e. the increase in average and maximal particles size; such an increase, according to particle-size distribution study can achieve 10-15 times.
3. Powder dispersity is a factor significantly affecting thermal behavior of the samples. In particular, the value of the exothermic effect due to powder dispersity decrease is much higher for samples manufactured from 10 μm aluminum fraction than for samples produced from 40 and 80 μm fraction. Similar statement can be done for silicon carbide samples – the decrease of the powder fraction from 14 to 7 μm gives rise to significant batch components interaction, as a result, silicon carbide oxidation is observed for the samples with higher SiC powder dispersity.

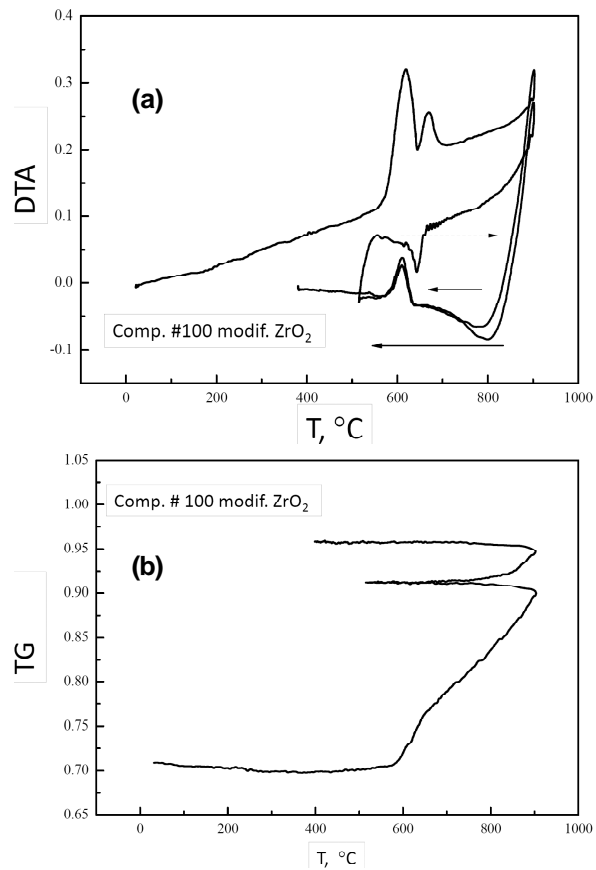


Fig. 10. Thermal analysis results for the composition 95 wt.% of the 14%BN26%SiC60%Al batch – 5 wt.% of nano-sized zirconia powder.

4. Another factor affecting thermal behavior of the samples is their pre-treatment: pressing, heating in air, and vacuum annealing also change samples thermal behavior.
5. Ternary Al-BN-SiC compositions chosen for manufacturing of nanomodified functional ceramics were shown to be very perspective since at proper powder dispersity and necessary pretreatment they provide significant interactions between system components.
6. Batch nanomodification by nanosized zirconia powder makes possible purposeful modification of the required final ceramics properties - thermal stability, chemical stability, and permanence of phase composition at high temperatures.

ACKNOWLEDGEMENT

This work was supported by the Russian Ministry of Education and Science (Contract 8025), as well as the St. Petersburg State University research grant 6.37.671.2013.

REFERENCES

- [1] *Ceramic Turbine gas Component Development and Characterization*, ed. by Mark van Roode, Mattison K. Ferber and David W. Richerson (ASME Press, New York, 2002).
- [2] V.G. Konakov, S. Seal, E.N. Solovieva, S.N. Golubev, M.M. Pivovarov, A.V. Shorokhov // *Rev. Adv. Mater. Sci.* **13** (2006) 71.
- [3] O.Yu. Kurapova, V.G. Konakov, S.N. Golubev, V.M. Ushakov and I.Yu. Archakov // *Rev. Adv. Mater. Sci.* **32** (2012) 112.
- [4] D.A. Ivanov-Pavlov, V.G. Konakov, E.N. Solovieva, V.M. Ushakov, N.V. Borisova. // *Journal of Nano Research* **6** (2009) 35.
- [5] A.V. Monin, E.G. Zemtsova, N.B. Shveikina and V.M. Smirnov // *Nanotechnologies in Russia* **7** (2012) 152.
- [6] Anatoly V. Soudarev and Vitaly. Yu. Tikhoplav, In : *Ceramic Turbine gas Component Development and Characterization*, ed. by Mark van Roode, Mattison K. Ferber and David W. Richerson (ASME Press, New York,2002), p. 683.
- [7] V.G. Konakov, A.V. Soudarev, N.F. Morozov and I.A. Ovid'ko, Russian Patent 2399601 C2, 19.11.2008.
- [8] V.G. Konakov, S.N. Golubev, E.N. Solovyeva, I.Yu. Archakov, N.V. Borisova and A.V. Shorokhov // *Materials Physics and Mechanics* **14** (2012) 1.
- [9] V.G. Konakov, N.V. Borisova, S.N. Golubev, O.Yu. Kurapova and V.M. Ushakov // *Vestnik SPBGU* 4(3) (2012) 65, In Russian.
- [10] I. Barin and O. Knacke, Thermochemical properties of inorganic substances (Dusseldorf, 1973).
- [11] Y. G. Gogotsi, A.G. Gogotsi and O.D. Scherbina // *Powder Metallurgy and Metal Ceramics* **25(5)** (1986) 388.
- [12] Y. G. Gogotsi, S.I. Sopenko and G.V. Trunov // *Problemy Prochnosty* **1** (1985) 69, In Russian.
- [13] A.V. Gunchenko // *Powder Metallurgy and Metal Ceramics* **29(12)** (1990) 964.